Convection-Driven Thermal and Mass Transfer in 3D Bioprinting: Micropore Formation and Heat Transfer in PCL and PLGA Scaffolds

Mihir Madhaparia

May 9, 2025

Abstract

Three-dimensional (3D) bioprinting enables the fabrication of tissue scaffolds crucial for regenerative medicine. For common extrusion-based methods using polymers like polycaprolactone (PCL) and poly(lactic-co-glycolic acid) (PLGA) dissolved in volatile solvents, the creation of essential microporosity relies heavily on solvent evaporation during and after printing. This evaporation process is fundamentally governed by coupled convective heat and mass transfer between the extruded filament and the surrounding environment. The rate of evaporation, dictated by factors such as ambient airflow velocity, temperature, and solvent vapor concentration, directly influences the final pore structure, including pore size, interconnectivity, and overall porosity. These architectural features are critical for subsequent cell infiltration, nutrient transport, and waste removal within the scaffold. This paper examines the principles of convection-driven transport phenomena in this context. It details how environmental parameters modulate the convective heat transfer coefficient (h), which supplies the energy for vaporization, and the mass transfer coefficient (h_m), which governs the rate of solvent vapor removal. The interplay between heat supply and mass removal determines the filament surface temperature and concentration gradients, thereby influencing polymer precipitation kinetics and the resulting microporous morphology. Furthermore, the pore structure established during this evaporative phase dictates the effective thermal conductivity (k_{eff}) of the solidified scaffold, impacting its thermal behavior during cell culture or in vivo application. Understanding and controlling the convective environment is therefore presented as a key strategy for optimizing scaffold microarchitecture and functional properties for tissue engineering applications.

1 Introduction

Regenerative medicine holds immense promise for repairing or replacing damaged tissues and organs, offering potential solutions for conditions ranging from traumatic injuries to degenerative diseases. A major challenge lies in creating biocompatible structures that can support cell growth and guide tissue formation, effectively mimicking the natural extracellular matrix (ECM). Three-dimensional (3D) bioprinting has emerged as a powerful technology to address this challenge, enabling the layer-by-layer fabrication of complex, patient-specific biological constructs, including tissue scaffolds [1]. Applications are diverse, spanning bone, cartilage, skin, and even

intricate structures for nerve tissue regeneration [8]. The success of these scaffolds hinges on their architecture, particularly their porosity.

This term paper focuses specifically on a common method within 3D bioprinting: extrusion-based printing using biodegradable polymers like polycaprolactone (PCL) and poly(lactic-co-glycolic acid) (PLGA) dissolved in volatile organic solvents, such as dichloromethane [3]. In this technique, the crucial microporous structure, essential for cell viability, nutrient diffusion, and waste removal [2], is primarily formed during and immediately after the printing process through the evaporation of the solvent from the extruded polymer solution filament. The resulting pores create the necessary void space for cells to reside and for essential biological transport processes to occur. The critical step governing the final scaffold architecture is this solvent evaporation process. The rate and dynamics of evaporation are dictated by fundamental principles of coupled heat and mass transfer occurring between the printed filament and its surrounding environment. This transport is predominantly driven by convection. Key environmental parameters influencing this process include the ambient air velocity (U), air temperature (T_{air}), and the concentration of solvent vapor in the air (related to humidity, C_∞). These factors significantly impact how quickly the solvent leaves the filament. For instance, rapid drying conditions might lead to the formation of a dense "skin" on the filament surface, potentially trapping residual solvent or resulting in smaller, less interconnected pores compared to slower, more controlled drying conditions [4]. Therefore, understanding and precisely controlling the convective heat and mass transfer during printing is paramount for optimizing scaffold properties like pore size distribution, interconnectivity, and ultimately, biological function.

Section 2 will introduce fundamental concepts relevant to transport in porous media, such as porosity, permeability, and effective diffusivity. Section 3 will detail the coupled heat and mass transfer mechanisms governing solvent evaporation at the filament surface. Section 4 will explore how manipulating convective parameters (airflow, temperature, ambient concentration) can be used to control pore formation, introducing relevant dimensionless numbers and correlations. Finally, Section 5 will discuss heat transfer within the solidified scaffold, characterized by its effective thermal conductivity, which is itself a consequence of the pore structure formed during the evaporation phase. The overarching goal is to provide a framework for understanding how the convective environment shapes scaffold microarchitecture and thermal properties.

2 Heat and Mass Transfer Fundamentals in Porous Scaffolds

2.1 Porosity, Permeability, and Diffusivity

Scaffolds are porous media, meaning transport phenomena differ from bulk materials. Key parameters include:

- **Porosity (ϕ)**: The fraction of void volume to total volume.

$$\phi = \frac{V_{void}}{V_{total}} \tag{1}$$

- **Permeability (K)**: A measure of the ability of a fluid to flow through the porous medium,

described by Darcy's Law for low Reynolds number, saturated flow [5]:

$$\vec{v} = -\frac{K}{\mu}\nabla P \tag{2}$$

where $\vec{v}$ is the Darcy velocity, μ is dynamic viscosity, and ∇P is the pressure gradient. The Brinkman equation can offer refinement by including viscous shear effects.

- **Effective Diffusivity (D_{eff})**: Diffusion in porous media is hindered by the solid matrix. D_{eff} accounts for porosity and tortuosity (τ), which represents the convoluted path molecules take [5]:

$$D_{eff} = \frac{\phi}{\tau}D \tag{3}$$

where D is the molecular diffusion coefficient in the fluid. Tortuosity quantifies the degree to which the diffusion path length is longer than the straight-line distance through the medium due to the complex pore structure.

2.2 Effective Thermal Conductivity

Heat transfer within the scaffold is governed by the effective thermal conductivity (k_{eff}). A simple volume-averaging model provides a basic estimate [6]:

$$k_{eff} = k_f\phi + k_s(1-\phi) \tag{4}$$

where k_f and k_s are the thermal conductivities of the fluid (air or culture medium within pores) and solid (polymer matrix) phases, respectively. It is important to note that this model is a simplification and may be insufficient when phase properties differ significantly or interfacial resistance is high. More complex models exist that account for pore geometry and phase distribution, but these require more detailed structural information.

3 Micropore Formation via Solvent Evaporation

In solvent-based bioprinting, micropores form as the volatile solvent evaporates from the extruded polymer solution filament. This process involves solvent diffusion from the filament's interior to the surface, phase change (liquid to vapor) at the surface, and subsequent convection of the solvent vapor away from the surface into the surrounding environment. The overall rate and dynamics are dictated by the coupled heat and mass transfer occurring at the filament surface.

- **Mass Transfer**: The molar rate of solvent evaporation ($\dot{m}$) is primarily driven by the difference between the solvent vapor concentration at the filament surface (C_s) and the concentration in the bulk ambient air (C_∞), facilitated by the convective mass transfer coefficient (h_m) [6]:

$$\dot{m} = h_m A(C_s - C_\infty) \tag{5}$$

Here, A is the filament surface area. C_s is related to the solvent's partial pressure at the surface, which depends on the surface temperature and the polymer-solvent thermodynamics,

while C_∞ depends on the ambient humidity and any solvent vapor accumulation. h_m encapsulates the efficiency of the convective flow in removing vapor from the surface boundary layer.

- **Heat Transfer**: Evaporation is an endothermic process requiring the latent heat of vaporization (L). This energy is primarily supplied by convective heat transfer from the warmer ambient air (T_{air}) to the cooler filament surface ($T_{surface}$), governed by the convective heat transfer coefficient (h) [6]:
$$q''_{conv} = h(T_{air} - T_{surface}) \tag{6}$$
where q''_{conv} is the convective heat flux (energy per unit area per unit time). Radiative heat transfer may also contribute, but is often secondary unless temperature differences are large or specific heating sources are used.

- **Energy Balance**: Under quasi-steady conditions, the energy supplied by convection must balance the energy consumed by evaporation:
$$q''_{conv} \approx \dot{m}L \tag{7}$$
Substituting the expressions for q''_{conv} and $\dot{m}$ highlights the coupling:
$$hA(T_{air} - T_{surface}) \approx h_m A(C_s(T_{surface}) - C_\infty)L \tag{8}$$
This balance determines the filament's surface temperature and the actual evaporation rate.

The interplay between the rate of heat supply and the rate of mass removal dictates the surface temperature and the solvent concentration gradient within the filament. These factors, in turn, influence the kinetics of polymer precipitation and phase separation as the solvent concentration drops below the solubility limit. Faster evaporation rates (promoted by high h, high h_m, low C_∞, high T_{air}) can lead to rapid solidification at the surface, potentially trapping solvent inside or resulting in smaller, less interconnected pores (a skin layer effect). Conversely, slower, controlled evaporation may allow more time for polymer chain rearrangement and phase separation mechanisms, potentially leading to larger, more defined, and interconnected pore structures [4]. Therefore, precise control over the convective environment is crucial for tailoring the final microporous architecture.

4 Controlling Pore Formation via Convection

As established, the final microporous structure is highly sensitive to the rate of solvent evaporation, which is governed by convective heat and mass transfer. Therefore, controlling the convective environment during printing offers a powerful means to tune scaffold morphology. Key control parameters include:

- **Airflow Velocity (U)**: Increasing the airflow velocity generally enhances both the heat (h) and mass (h_m) transfer coefficients by thinning the thermal and concentration boundary layers adjacent to the filament surface. This leads to faster evaporation. Conversely, printing in still air or a low-flow enclosure reduces convection and slows evaporation.

- **Ambient Temperature (T_{air})**: Higher T_{air} increases the thermal driving force ($T_{air} - T_{surface}$) for heat transfer to the filament, supplying more energy for evaporation. It also increases the saturation vapor pressure of the solvent, potentially increasing C_s and the mass transfer driving force ($C_s - C_\infty$).
- **Ambient Humidity/Solvent Concentration (C_∞)**: Increasing the concentration of solvent vapor in the ambient air (e.g., by partially enclosing the print chamber) reduces the driving force for mass transfer, thereby slowing evaporation. Controlling humidity (for aqueous solvents) acts similarly.
- **Print Chamber Design**: Enclosing the print area allows for better stabilization and control of temperature, airflow, and ambient vapor concentration.

Quantifying the convective coefficients (h, h_m) is essential for predictive modeling and process optimization. Standard correlations, often expressed using dimensionless numbers like the Nusselt number ($Nu = hx/k$) for heat transfer and the Sherwood number ($Sh = h_m x/D_{AB}$) for mass transfer, relate these coefficients to fluid properties and flow conditions (e.g., Reynolds number $Re = \rho U x/\mu$, Prandtl number $Pr = \mu c_p/k$ for heat; Schmidt number $Sc = \mu/(\rho D_{AB})$ for mass) [6]. For instance, forced convection over a flat plate in laminar flow ($Re_x < 5 \times 10^5$) can be approximated by:

$$Nu_x = 0.332 Re_x^{1/2} Pr^{1/3} \quad (Pr \geq 0.6) \tag{9}$$

$$Sh_x = 0.332 Re_x^{1/2} Sc^{1/3} \quad (Sc \geq 0.6) \tag{10}$$

where x is the distance along the plate, k is thermal conductivity, D_{AB} is mass diffusivity, ρ is density, U is velocity, μ is dynamic viscosity, and c_p is specific heat.

However, applying such simplified correlations (developed for ideal geometries like flat plates or cylinders in uniform flow) to the complex geometry of a 3D printed filament within a potentially intricate airflow pattern inside a printer chamber is a significant approximation. The actual local transfer coefficients can vary substantially over the filament surface. More accurate predictions typically require computational fluid dynamics (CFD) simulations that solve the governing flow, heat, and mass transfer equations numerically for the specific geometry and boundary conditions. Nevertheless, these correlations provide valuable scaling relationships and highlight the key parameters influencing convective transport.

The heat and mass transfer analogies, such as the Chilton-Colburn analogy, provide a practical link between the transfer coefficients [6]:

$$j_H = \frac{Nu_x}{Re_x Pr^{1/3}} = \frac{C_f}{2} = \frac{Sh_x}{Re_x Sc^{1/3}} = j_M \tag{11}$$

Here, j_H and j_M are the Colburn j-factors for heat and mass transfer, respectively, and C_f is the friction factor. This analogy, valid primarily for turbulent flows where momentum, heat, and mass boundary layers develop similarly (and often approximated for laminar flows when $Pr \approx Sc$), implies that if one transfer coefficient (e.g., h) or the friction factor can be measured or estimated, the other coefficients (e.g., h_m) can be inferred. This is particularly useful as heat transfer (h) is often easier to measure experimentally than mass transfer (h_m).

(See Figure 1 for examples of resulting scaffold microstructures).

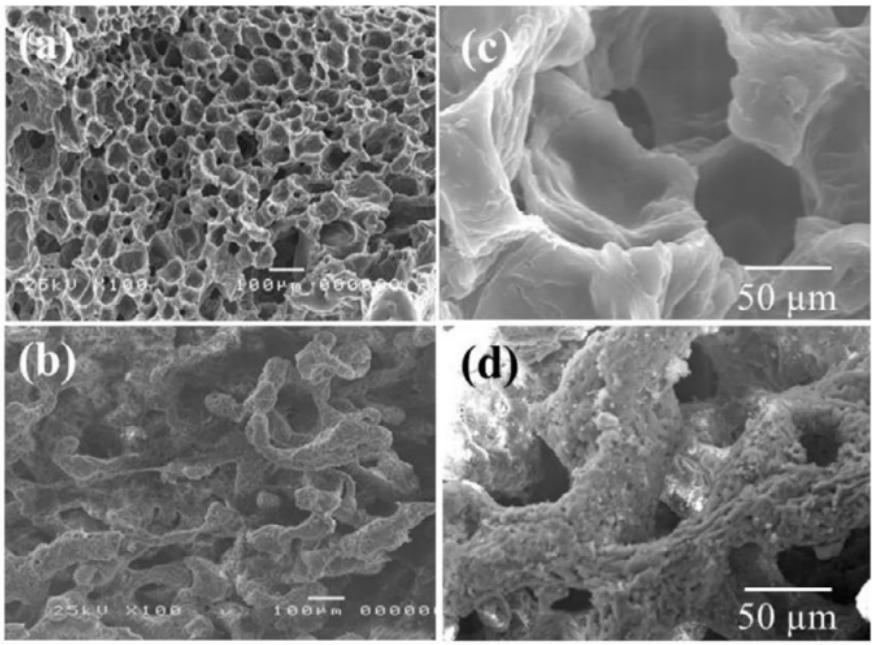

Figure 1: Representative SEM Micrographs of Microporous PCL/PLGA Scaffolds at different magnifications. (a,c represent PCL; b,d represent PLGA). Varying convective conditions during fabrication can lead to differences in pore size, shape, and interconnectivity seen in such images.

5 Heat Transfer in Solidified Scaffolds

Once the solvent has fully evaporated and the polymer scaffold has solidified, the primary mechanism of heat transfer within the scaffold structure shifts from convection/evaporation-dominated transport to conduction through the porous solid matrix and the fluid filling the pores. The overall ability of the scaffold to conduct heat is characterized by its effective thermal conductivity, k_{eff} (Eq. 4).

The temperature distribution within the solidified scaffold, particularly important when cells are cultured within it or when it is implanted in vivo, is governed by the steady-state heat diffusion equation:

$$\nabla \cdot (k_{eff} \nabla T) + \dot{q}_{gen} = \rho c_p \frac{\partial T}{\partial t} \tag{12}$$

where $\dot{q}_{gen}$ represents any internal heat generation (e.g., metabolic heat from cells, though often negligible on the macro scale) and the right side is zero for steady state. For simple 1D steady-state conduction without generation, this reduces to Fourier's Law:

$$q'' = -k_{eff} \frac{dT}{dx} \quad \text{(constant)} \tag{13}$$

The value of k_{eff} is crucial. It depends not only on the thermal properties of the solid polymer (k_s) and the pore-filling fluid (k_f) but also significantly on the porosity (ϕ), pore size, shape, interconnectivity, and tortuosity (τ) – the very architectural features determined during the solvent evaporation phase. Thus, controlling the convective drying process directly impacts the subsequent

thermal performance of the solidified scaffold.

At the boundaries of the scaffold, heat transfer occurs via convection, linking the internal temperature field to the external environment (T_∞) through Newton's Law of Cooling:

$$-k_{eff}\frac{\partial T}{\partial n}\bigg|_{boundary} = h(T_{boundary} - T_\infty) \tag{14}$$

where $\partial T/\partial n$ is the temperature gradient normal to the boundary, and h is the convective heat transfer coefficient characterizing the external fluid flow. This boundary condition highlights the continued importance of convection in determining the overall thermal state of the scaffold even after solidification.

Minimizing thermal gradients (∇T) within cell-laden scaffolds during culture or post-implantation is often critical for ensuring cell viability and function [7]. Large temperature variations can induce stress, trigger apoptosis (programmed cell death), or lead to non-uniform cell behavior. Scaffolds with low k_{eff} (often associated with high porosity) can be prone to developing larger internal temperature gradients if subjected to external heat fluxes or internal metabolic heating. Therefore, understanding how the fabrication process influences k_{eff} and how the scaffold interacts thermally with its environment is vital for successful tissue engineering applications.

6 Summary Table of Key Transport Concepts

Table 1: Summary of Key Transport Concepts in Bioprinting

Concept	Equation (Example)	Key Parameters	Relevance in Bioprinting	Reference
Porosity	$\phi = V_{void}/V_{total}$	ϕ	Defines void space for cells, nutrients	-
Permeability	$\vec{v} = -(K/\mu)\nabla P$	K	Governs fluid flow (nutrients, waste) through scaffold	[5]
Eff. Diffusivity	$D_{eff} = (\phi/\tau)D$	D_{eff}, τ	Controls solute transport rate within pores	[5]
Eff. Thermal Cond.	$k_{eff} = k_f\phi + k_s(1-\phi)$	k_{eff}	Determines heat distribution in solidified scaffold	[6]
Conv. Mass Tx	$\dot{m} = h_m A(C_s - C_\infty)$	h_m, C_s, C_∞	Drives solvent evaporation, influencing pore formation	[6]
Conv. Heat Tx	$q'' = h(T_{air} - T_{surf})$	h, T_{air}, T_{surf}	Supplies energy for evaporation, coupling heat/mass tx	[6]
Heat/Mass Analogy	$j_H = j_M$	h, h_m, Pr, Sc	Relates heat and mass transfer coefficients	[6]

7 Conclusion

Convection-driven thermal and mass transfer are critical determinants of micropore structure in 3D bioprinted scaffolds made from PCL, PLGA, and similar materials using solvent-based methods. By understanding and controlling the underlying physics—solvent diffusion, evaporation rates influenced by h and h_m, and heat exchange governed by convective conditions (T_{air}, C_∞, U)—engineers can tailor scaffold porosity, permeability, and effective thermal conductivity (k_{eff}). This control over architecture and properties is essential for advancing regenerative medicine applications, from neural repair to bone regeneration [1, 2]. Furthermore, understanding heat transfer in the solidified scaffold is crucial for managing the thermal environment of embedded cells. Future work may involve integrating real-time monitoring and feedback control systems, potentially guided by AI, into bioprinters to achieve even greater precision in scaffold fabrication by actively managing the convective environment.

References

[1] Murphy, S.V., and Atala, A. (2014). 3D bioprinting of tissues and organs. *Nat. Biotechnol.*, 32(8):773-785.

[2] Melchels, F.P. et al. (2012). Additive manufacturing of tissues and organs. *Prog. Polym. Sci.*, 37(8):1079-1104.

[3] Nair, L.S. and Laurencin, C.T. (2007). Biodegradable polymers as biomaterials. *Prog. Polym. Sci.*, 32(8-9):762-798.

[4] Ozbolat, I.T. and Hospodiuk, M. (2016). Current advances and future perspectives in extrusion-based bioprinting. *Biomaterials*, 76:321-343.

[5] Bear, J. (1988). *Dynamics of Fluids in Porous Media*. Dover Publications.

[6] Bergman, T.L., Lavine, A.S., Incropera, F.P., DeWitt, D.P. (2011). *Fundamentals of Heat and Mass Transfer*. 7th Ed. Wiley.

[7] Buwalda, S.J. et al. (2014). Hydrogels in biomedical applications: From tissues to therapeutic systems. *J. Control. Release*, 190:254-273.

[8] Wang, X., et al. (2016). Engineering aligned poly(lactic acid)-poly(ε-caprolactone)/collagen scaffolds for nerve tissue regeneration. *Biofabrication*, 8(3):035010.